Performance Analysis of Ejector Cycles for Separate Sensible and Latent Cooling in Air Conditioning

Jim Carow
Optimized Thermal Systems, Inc., carow@optimizedthermalsystems.com

Daniel Bacellar
University of Maryland, College Park

Cara Martin
Optimized Thermal Systems, Inc.

Performance Analysis of Ejector Cycles for Separate Sensible and Latent Cooling in Air Conditioning

James CAROW[1*], Daniel BACELLAR[2], Cara MARTIN[1]

[1]Optimized Thermal Systems, Inc.
Beltsville, MD, USA

[2]University of Maryland, College Park
College Park, MD, USA

* Corresponding Author
Email: carow@optimizedthermalsystems.com

ABSTRACT

While the overall system efficiency of split air conditioning (AC) systems has improved over the last three decades, residential air handling units (AHUs) used in those systems have essentially stayed the same in size, shape, form, and efficiency. Incremental improvements have been made to AHUs to address safety, functionality, and energy-efficiency concerns, however, their overall structure has remained the same. A promising technology that addresses fundamental challenges with conventional cycle efficiencies are ejector-based cycles, more commonly employed in refrigeration applications, but with great potential in AC systems as well. An ejector employed as an expansion device can recover expansion losses, boost pressure, and facilitate a dual evaporator system. This paper presents four categories of ejector enhanced vapor compression cycles (VCCs) leading to seven potential system concepts: standard two-phase ejector, two variants of condenser outlet split (COS), diffuser outlet split (DOS), and three variants of separator outlet split (SOS). The concepts were investigated via numerical model studies and two promising ejector enhanced cycles for a residential AC application emerged: COS and DOS. The COS and DOS ejector enhanced cycles improved seasonal energy efficiency ratio (SEER) by 4%–8% above a 15 SEER baseline AC system and improved the total coefficient of performance (COP) by 9%–11%. With the COS or DOS ejector enhanced cycles, losses quantified by exergy destruction were reduced by up to 18%.

1. INTRODUCTION

Residential air handling units (AHUs) used in split air conditioning systems, have essentially stayed the same in size, shape, form, and efficiency over the past 30+ years. While incremental improvements have been made to address safety, functionality, and energy-efficiency concerns, the overall structure has remained the same. Significant change is needed to develop a next generation design that can more readily address the increasing energy challenges of tomorrow. This includes reducing the contribution of HVAC systems on overall energy consumption, which accounted for 51% of the total energy for U.S. residential households in 2015 (U.S. EIA, 2018).

Irreversibilities due to the compression process and finite temperature difference heat transfer in the heat exchangers (HX's) make up the greatest contributions to system-level performance reduction. In recent years, increasing needs to improve air conditioner (AC) and heat pump (HP) efficiency have led manufacturers to improve condenser performance as a means of reducing system pressure lift and therefore compressor power consumption.

Such improvements have been effective and are manifest in an obvious increase in AC outdoor unit size in residential systems over time. Improvements to indoor unit performance have not been so easy to achieve; the function of an AC indoor unit is not only to reduce temperature, but also to dehumidify the space, requiring an evaporating temperature below the incoming air dewpoint. If a more effective evaporator were employed, approach temperatures could be reduced and the compressor would consume less power, but the AHU would no longer adequately dehumidify the space. Separate sensible and latent cooling (SSLC), where the sensible cooling process can be performed at a higher temperature and efficiency, and latent cooling (dehumidification) is performed by a separate process, has been investigated previously (Ling et al. 2010).

Kornhauser (1990) listed major thermodynamic losses in a vapor compression cycle (VCC): heat exchange across a temperature difference in the evaporator and condenser, compressor inefficiency, heat exchange from superheated vapor at the compressor discharge, and the throttling process in the expansion valve. Kornhauser introduced the idea of an ejector used as an expansion device to recover intrinsic expansion losses and showed the potential for increased COP, and decreased compressor displacement and pressure ratio.

Indeed, an ejector employed as an expansion device can recover expansion losses, boost pressure, and based on system configuration, facilitate a dual evaporation temperature system. A dual evaporator system represents a type of SSLC system. Inspired in part by Lawrence and Elbel (2013), four categories of ejector enhanced vapor compression cycles were investigated, leading to seven potential system concepts: standard two-phase ejector, two variants of COS, one DOS variant, and three variants of SOS. The cycles included two-phase, saturated, and superheated vapor conditions in the ejector.

2. EJECTOR ENHANCED VAPOR COMPRESSION CYCLES

2.1 Form and Function of an Ejector

A conventional ejector is a passive component with no moving parts. Essentially an ejector is a pair of nozzles, usually co-annular, a mid-section which acts as a mixing chamber, and a diffuser.

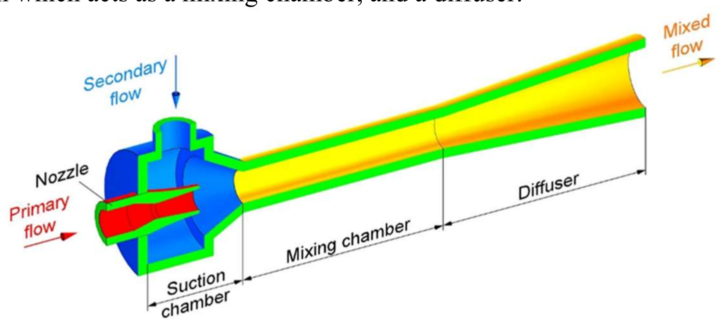

Figure 1: Cut-away view of an ejector (ERTC, 2014).

The function of an ejector is two-fold: to entrain the flow of fluid, and to increase a fluid's pressure. A high-pressure fluid enters the motive nozzle, expands, and creates suction, which entrains the flow of fluid into the secondary nozzle. The fluids then mix in the mixing chamber and exit through a diffuser. The diffuser compresses the fluid and increases the pressure of the exiting fluid mixture above the pressure level of the entrained secondary flow. In this way an ejector works as both an expansion device and a refrigerant pump.

An ejector inherently merges two flow streams and when used in conjunction with components which divide flows, such as tees or a liquid-vapor separator, various alternative VCCs and system configurations can be created depending on the placement of the ejector with respect to the other components. These configurations give rise to differences in the refrigerant states at the ejector. Configurations are possible which yield two-phase, superheated vapor, or saturated vapor states. Importantly, these system configurations also allow for cycles with dual evaporators.

2.2 Cycle Configurations

Schematics of the ejector enhanced VCC configurations are shown in Figure 2. The standard two-phase ejector cycle employs a single evaporator and an ejector replaces the typical expansion valve in the system as shown in Figure 2a. The primary ejector flow is the high-pressure liquid leaving the condenser at point 3. The vapor at point 10, leaving the evaporator, is entrained by the secondary nozzle of the ejector. The ejector outlet flow at point 7 has a pressure which is higher than the evaporation pressure due to the ejector pressure lift. A liquid-vapor separator feeds vapor to the compressor and liquid to a metering valve. The metering valve further expands the refrigerant to the evaporator.

In contrast to the standard two-phase ejector cycle, the following six cycles, which are of types COS, DOS, or SOS systems; all utilize dual evaporators. In the case of these dual evaporator cycles the schematics show the air flow to the evaporators in series, with the high temperature evaporator receiving air flow first followed by the low temperature evaporator.

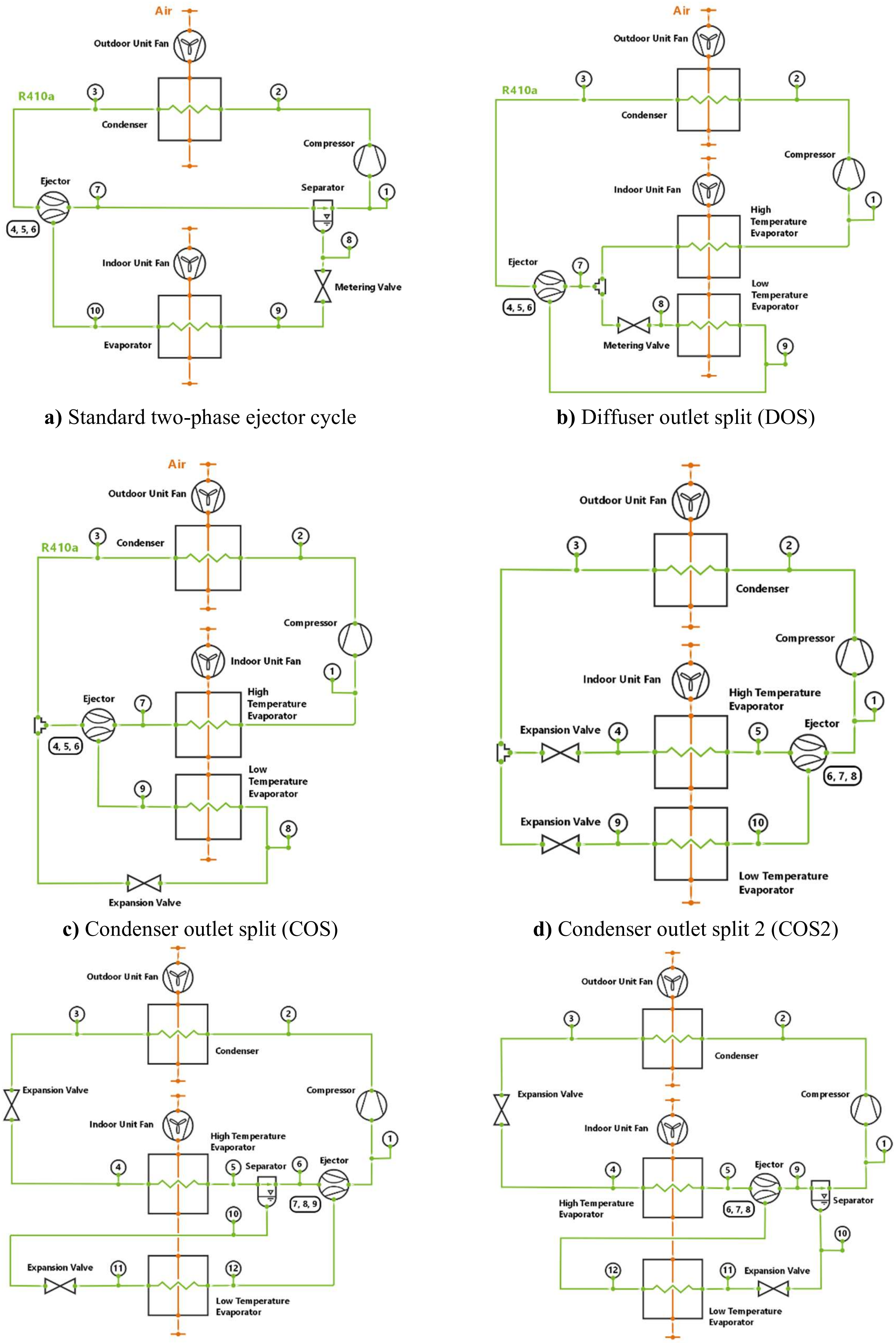

a) Standard two-phase ejector cycle

b) Diffuser outlet split (DOS)

c) Condenser outlet split (COS)

d) Condenser outlet split 2 (COS2)

e) Separator outlet split (SOS)

f) Separator outlet split 2 (SOS2)

Figure 2: Ejector enhanced vapor compression cycle configurations.

The two-phase DOS system was studied by Lawrence & Elbel (2013) and is shown in Figure 2b. The DOS system uses the ejector as an expansion device. The refrigerant flow division occurs after the ejector at the diffuser outlet point 7, where the flow is routed to the high temperature evaporator then through a metering valve which reduces the pressure to the low temperature evaporator inlet at point 8. The two evaporators see parallel refrigerant flow. The metering valve and low temperature evaporator form a refrigerant flow recirculation loop. No liquid-vapor separator is employed.

Lawrence & Elbel (2013) detailed the two-phase COS shown in Figure 2c. The name stems from the fact that the refrigerant flow splits after the condenser. In this system there are two evaporators in parallel in refrigerant flow. An ejector is utilized used as the expansion device for the high temperature evaporator and an expansion valve is employed for the low temperature evaporator. There is no liquid-vapor separator. The second evaporator operates at a lower temperature and has a lower refrigerant mass flow rate. The high temperature evaporator sees the lifted pressure at point 7 and its refrigerant flow rate is that of the ejector diffuser outlet.

Another system which divides the refrigerant flow after the condenser is the COS2, described by Lee et al. (2000). In contrast to the COS cycle, where the ejector flows were two-phase, the COS2 cycle is a superheated vapor ejector cycle. The system schematic can be seen in Figure 2d. A pair of expansion valves are employed, and the ejector is placed downstream of a pair of evaporators which are fed refrigerant flow from the condenser. No liquid-vapor separator is used. Both evaporator outlet flows, points 5 and 10 (Figure 2d), as well as the ejector flows, are superheated.

Tomasek & Radermacher (1995) studied the SOS ejector system in a refrigeration application, see Figure 2e for the schematic. The system uses two expansion valves, and the two evaporators are in series in the refrigerant flow. A liquid-vapor separator divides the refrigerant flow, points 6 and 10 (Figure 2e), and feeds the ejector and the low temperature evaporator. The ejector diffuser outlet enters the compressor. The SOS system refrigerant flows driving the ejector are saturated vapor.

The SOS2 system, shown in Figure 2f, was analyzed by Wang et al. (2014). Two expansion valves are utilized, and the two evaporators are in series in refrigerant flow. The branch in the refrigerant flow occurs at the liquid-vapor separator which feeds vapor to the compressor at point 1, and liquid to the second expansion valve at point 10. The primary flow to the ejector is two-phase refrigerant and the secondary flow is either saturated or superheated vapor.

3. NUMERICAL MODELING

3.1 Ejector Modeling

The ejector model followed the approach from Kornhauser (1990). Values for the nozzle & diffuser efficiencies were those used by Lawrence & Elbel (2013): η_{mn}= 0.80 [-], η_{sn}= 0.80 [-], η_{diff}= 0.75 [-]. The ejector motive and secondary nozzle efficiencies are defined as:

$$\eta_{mn} = \frac{h_{primary} - h_{mn}}{h_{primary} - h_{mn,s}}, \qquad \eta_{sn} = \frac{h_{secondary} - h_{sn}}{h_{secondary} - h_{sn,s}} \tag{1}$$

and ejector diffuser efficiency is:

$$\eta_{diffuser} = \frac{h_{diffuser} - h_{mix}}{0.5 \cdot V_{mix}^2} \tag{2}$$

The suction pressure fraction of the ejector, n, relates the mixing pressure of the ejector to the pressure at the inlet of the secondary nozzle inlet pressure. This relationship is given in Equation (3):

$$P_{mix} = (1 - n) \cdot P_{secondary} \tag{3}$$

The diffuser exit flow is the sum of the motive and secondary nozzle flows:

$$\dot{m}_{diffuser} = \dot{m}_{motive} + \dot{m}_{secondary} \tag{4}$$

The ejector mass flow ratio, r, is the ratio of the motive nozzle flow to the diffuser exit flow:

$$\mathrm{r} = \frac{\dot{m}_{motive}}{\dot{m}_{diffuser}} \tag{5}$$

Generally, the values of the parameters *n* and r were found by minimizing the sum of squares error in the energy balance. In the case of two-phase ejector cycles, Kornhauser (1990) had previously shown that the diffuser exit quality is equal to the ejector mass flow ratio. Therefore, in the case of the two-phase ejector cycles, in addition to the energy balance error, the difference between the diffuser outlet quality and the ejector mass flow ratio was used in the objective function in a sum of squares minimization in order to match the diffuser exit vapor quality.

3.2 Vapor Compression System Modeling

Detailed baseline modeling included heat exchanger and system-level steady-state models with proprietary software tools: CoilDesigner® (Jiang et al. 2006) to model heat exchangers, and VapCyc® (Winkler et al. 2008) to model the baseline vapor compression system. The VapCyc® model made use of the CoilDesigner® heat exchanger models as well as a 10-coefficient compressor model with coefficients provided by the compressor manufacturer.

Since an ejector component model was not available in VapCyc®, additional modeling was accomplished in EES®-Engineering Equation Solver (Klein 2020). First, two types of baseline models were implemented: a simplified model of the VCC with no air side details, and a more detailed model including the air side of the heat exchangers.

The simplified EES® models incorporated the following assumptions: fixed evaporator capacity and temperature, fixed condensing temperature, prescribed compressor mass flow and isentropic efficiency, prescribed superheat and subcooling.

To develop representations of the airside of the heat exchangers for use in the more detailed EES® models, parametric runs were conducted in CoilDesigner® for each heat exchanger over a range of expected conditions. Regression-based correlations of the product of the total heat transfer coefficient and area (UA) for heat exchangers were developed. In EES®, the log-mean temperature (LMTD) method, and an analogous log mean humidity ratio method, were employed using the regression-based UA value correlations to calculate sensible and latent cooling capacities. Evaporator UA value correlations were found from regression of parametric runs over a range of refrigerant pressures, mass flows, and vapor qualities. Condenser UA value correlations were found from regression of parametric runs over a range of refrigerant mass flows and outdoor air inlet temperatures. Models for each ejector-based cycle were implemented in EES®. UA correlations derived for an existing A-coil were used for the baseline and standard ejector cycles, while for dual evaporator cycles UA correlations were derived for a single A-coil slab and employed for each evaporator.

Isentropic and volumetric efficiencies obtained from the baseline model were used as prescribed compressor efficiencies in other models. The detailed EES® system model had the following inputs: indoor and outdoor unit inlet air temperatures, humidities, air flow rates, and fan powers; compressor displacement, speed, and efficiencies; heat exchanger UA value correlation coefficients, superheat & subcooling temperatures, refrigerant side pressure losses.

3.3 Model Verification

Simplified EES® models for baseline, standard two-phase ejector, COS, and DOS cycle cases were verified against results from Lawrence & Elbel (2013) for the ‘realistic’ case with R134a as the refrigerant. Results for COP and mass flows for the ejector nozzles and diffuser were compared and errors were typically zero, with the following exceptions: standard two-phase ejector COP differed by 2.2% and secondary nozzle mass flow differed by 4%, and DOS cycle diffuser mass flow differed by 1.7%.

For the detailed vapor compression baseline system model, results from EES® were compared with results from a VapCyc® model for one choice of outdoor temperature. Differences in capacity, compressor power, compressor COP, and total COP ranged from -0.06% to 2.41%.

4. RESULTS

4.1 Results of simplified models

The working fluid was chosen to be R410A as this work focused on improving the performance of an existing commercially available system. With R410A as the refrigerant, the models for the concept cycles were evaluated and compared against a baseline four-component VCC and a VCC with dual evaporators. The COP and compressor compression ratio (CR) for these systems, normalized by the baseline and ordered left to right from highest to lowest COP, are shown in Figure 3. In agreement with the analysis from Lawrence and Elbel (2013), the COP of the standard two-phase ejector, COS, and DOS cycles were all found to be equivalent. The standard two-phase ejector, COS, and DOS cycles performed 7.3% better than baseline. Reduced CR leads to improved COP due to the pressure lift generated by the ejector. The dual evaporator VCC had the lowest COP of any cycle considered, 13.4% lower than baseline. The other candidate cycles performed worse than baseline, but better than the dual evaporator VCC.

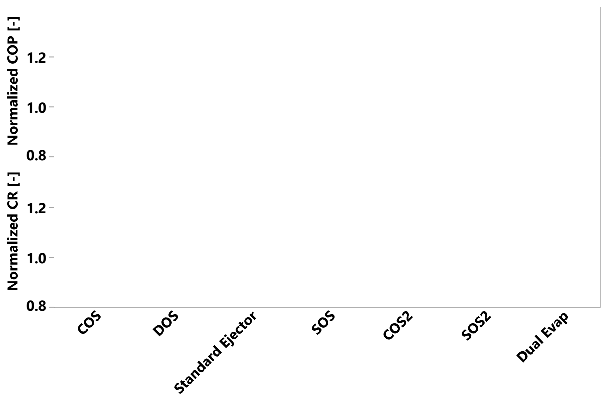

Figure 3: Normalized COP & CR for all systems.

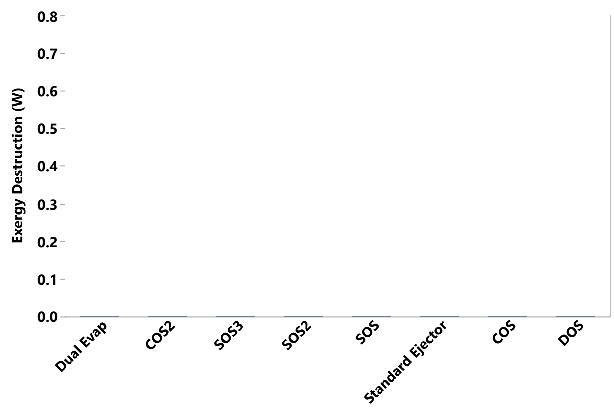

Figure 4: Exergy destruction in the AHU.

Model runs and analysis were repeated for the baseline and standard two-phase ejector cycle with R290 (propane) and R600a (isobutane) as the refrigerants, which have higher expansion losses than R410A. Analysis showed the ejector provided an additional 2 to 4% COP improvement above R410A with these natural refrigerants.

In addition to the traditional thermodynamic analysis of energy balances and calculation of performance criteria, a Second Law Analysis was performed on the baseline and each candidate system using exergy balances on refrigerant side only, which allowed a component-level accounting of losses due to irreversibilities. Exergy is a measure of the availability or 'usability' of energy and irreversibility is the loss of exergy. Exergy is a relative metric and is defined with reference to 'dead' state which is in thermodynamic equilibrium. The environmental state used was: $T_o = 25$ °C and $P_o = 101.325$ kPa. The enthalpy at this state is represented by h_o, and entropy by s_o. Specific exergy is defined in Equation (6), and the rate of exergy destruction by Equation (7):

$$\phi = h - h_o - T_o \cdot (s - s_o) \tag{6}$$

$$\dot{\Phi}_{dest} = \dot{Q}\left(1 - \frac{T_o}{T}\right) - \dot{W} + \sum \dot{m}_{in}\,\phi_{in} - \sum \dot{m}_{\text{out}}\,\phi_{\text{out}} \tag{7}$$

where, $\dot{Q}$ is capacity, $\dot{W}$ is work input, and $\dot{m}$ is mass flow rate.

Results of the refrigerant side exergy analysis are shown above in Figure 4, with the exergy destruction of each AHU component shown stacked. The total exergy destruction, represented by the height of the bars, reflects a performance metric for the AHU. The bars are ordered from highest to lowest exergy destruction. As expected, the dual evaporator has the highest exergy destruction with a significant portion coming from the expansion valves. In the case of the ejector cycles, the ejector accounts for some exergy destruction, however, the expansion losses can be seen to be lower in every case. The standard ejector cycle showed reduced expansion losses, however, the best performing cycles from this standpoint were the COS and DOS.

4.2 Evaluation of Selected Ejector Enhanced Concepts

The standard two-phase ejector, COS, and DOS cycles were selected for further analysis with the detailed modeling approach with R410A as the refrigerant. The baseline system was composed of a 10.55 kW (3 ton) residential AHU paired with an appropriate outdoor unit. The system was rated as nominal 15 SEER / 8.8 HSPF based on DOE energy standards to take effect in 2023 (EERE 2017).

Based on the AHRI Standard 210/240 (AHRI 2019), simulations were conducted at three different condenser air inlet temperatures: 27.8°C (82°F), 35°C (95°F), and 43.33°C (110°F); and 40% relative humidity (RH) to represent different outdoor ambient conditions. The indoor ambient condition, which is the evaporator air inlet condition, was kept constant at 26.7°C (80°F) and 50% RH. Total COP used in the detailed analysis included the effect of capacity loss and the parasitic power of the indoor and outdoor blower/fan motors.

To match each cycle's cooling capacity to the respective baseline case, the compressor displacement for each alternative cycle was modified by a scaling factor, where a value of one represents the baseline. A sum of squares error minimization approach was used to find the appropriate value of the compressor scaling parameter and iterated during model runs. Results are shown in Table 1. Across the three outdoor temperatures the standard ejector cycle compressor displacement ranged from 93 to 97%, COS cycle compressor displacement ranged from 88 to 96%, and DOS cycle ranged from 89 to 93% of baseline. Ejector pressure lift allows the compressor displacement to be reduced and the same cooling capacity as the baseline to be obtained.

The effect of the ejector on the compressor suction temperatures is shown in Table 2. The ejector increased the suction temperature above baseline for all ejector cycles and all ambient temperature cases. The largest temperature increase was observed in the DOS cycle, followed by the COS cycle, lastly the standard two-phase ejector cycle. These temperature increases correspond with reduced approach temperatures in the high temperature evaporator.

Table 1: Compressor scaling factor.

Cycle	Ambient Temperature [°C]		
	28	**35**	**43.33**
Baseline	1.00	1.00	1.00
Standard Ejector	0.97	0.93	0.93
COS	0.96	0.92	0.88
DOS	0.93	0.91	0.89

Table 2: Suction temperatures.

Cycle	Ambient Temperature [°C]		
	28	**35**	**43.33**
Baseline	10.2	10.8	11.7
Standard Ejector	11.5	13.3	15.4
COS	16.5	18.5	20.6
DOS	17.6	18.8	20.8

The sensible heat ratio (SHR) from the baseline model cases ranged from 0.76 to 0.81. Of interest are the SHR values for the high and low temperature evaporators in the COS and DOS cycles. The SHR for each evaporator in the COS and DOS cycles are shown in Figure 5, represented by points and the trend for each evaporator represented by a curve. The higher the outdoor ambient temperature, the more the high-temperature evaporator acted as a sensible heat exchanger and the less the low-temperature evaporator acted as a latent heat exchanger. The DOS cycle high-temperature evaporator tended to have higher SHR compared to the COS cycle. The low-temperature evaporators operated with lower SHR ranging from 0.56 to 0.68, however, they are not acting solely as latent heat exchangers. This suggests there is room for design improvement in ejector enhanced systems to advance further towards a completely decoupled sensible and latent heat system.

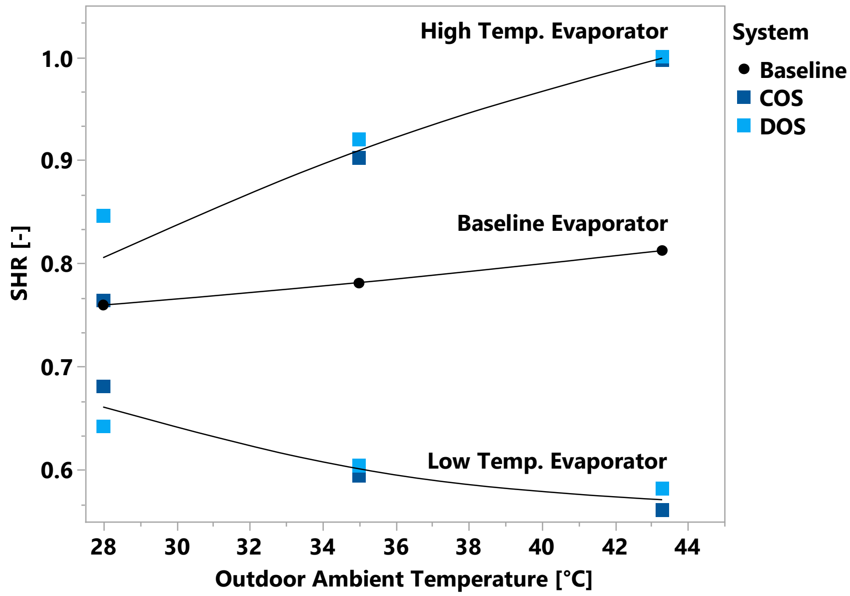

Figure 5: SHR of COS & DOS Cycle Evaporators.

The percent change in compressor power, CR, and COP total for the standard two-phase ejector, COS, and DOS cycles at each outdoor ambient temperature are shown in Figure 6. The percent improvement in COP total for the COS & DOS cycles ranged from 8 to 11% across the ambient temperatures. The standard two-phase ejector cycle performed comparatively poorer, with COP total improvements of 2 to 7% across the ambient temperatures. The improvement in COP total in these cycles was driven by the reduction in compressor power due to a reduction in compression ratio enabled by the ejector.

The DOS cycle was found to perform most favorably with an 8% increase in SEER, followed by the COS cycle with a 4% increase, as shown in Figure 7. The difference in SEER between the COS and DOS cycles was due to total power consumption for the DOS cycle being 3.4% lower than the COS cycle at the 28°C rating point. The standard ejector cycle showed only a 1% increase in SEER over the baseline.

5. CONCLUSIONS

Four categories of ejector enhanced VCCs with seven total system concepts were evaluated via simplified numerical model studies and three concepts emerged as beneficial. The baseline case and three ejector enhanced concepts were further studied with detailed models which included both the refrigerant and air side of the systems. Based on detailed models two promising ejector enhanced cycles for this AC application emerged: COS and DOS. The COS and DOS ejector enhanced cycles improved SEER by 4%–8% above a 15 SEER baseline AC system and improved the total coefficient of performance (COP) by 9%–11%. With the COS or DOS ejector enhanced cycles, losses quantified by exergy destruction within the AHU were reduced by up to 18%. As described in Lawrence & Elbel (2013) the COS and DOS ejector cycles are advantageous compared to other ejector enhanced cycles because they do not require a liquid-vapor separator. Future work should focus on application of alternative refrigerants and physical prototyping to better understand ejector performance in off-design conditions.

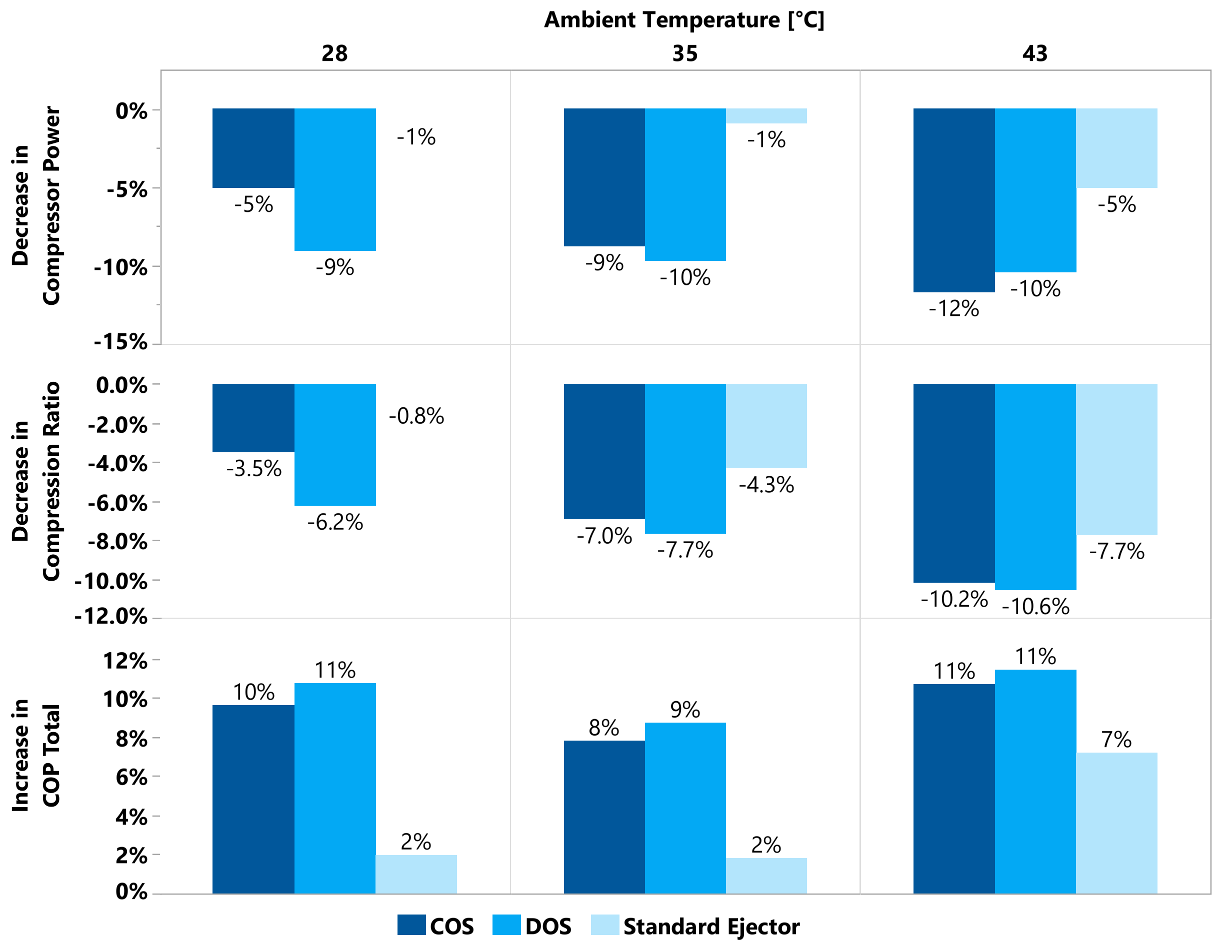

Figure 6: Comparison of compressor power, CR, and total COP.

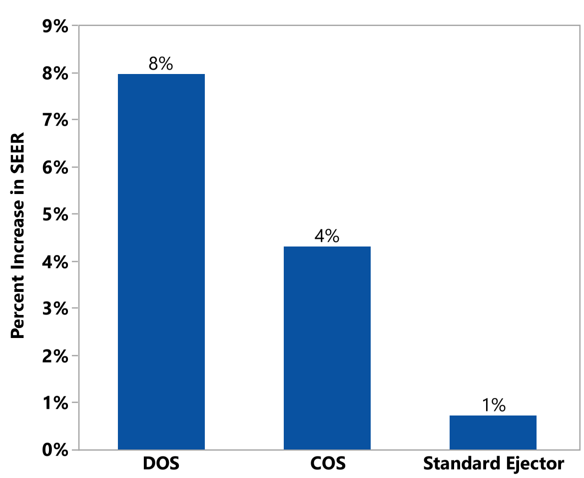

Figure 7: Comparison of SEER.

NOMENCLATURE

h	specific enthalpy	(kJ/kg)	**Subscript**	
$\dot{m}$	refrigerant mass flow	(kg/s)	dest	destroyed
n	suction pressure fraction	(–)	mix	mixing
P	pressure	(kPa)	mn	motive nozzle
$\dot{Q}$	capacity	(kW)	o	dead state
r	mass flow ratio	(–)	sn	secondary nozzle
s	specific entropy	(kJ/kg-K)	s	isentropic
T	temperature	(°C or K)		
$\dot{W}$	work input	(kW)		
η	efficiency	(–)		
ϕ	specific exergy	(kJ/kg)		
$\dot{\phi}$	rate of exergy destruction	(kW)		

REFERENCES

AHRI. (2019). Air-Conditioning, Heating, & Refrigeration Institute (AHRI). Retrieved from AHRI Releases December 2019 U.S. Heating and Cooling Equipment Shipment Data website: http://www.ahrinet.org/App_Content/ahri/files/Statistics/Monthly Shipments/2020/February_2020.pdf

EERE. (2017). 2017-01-06 Energy Conservation Program: Energy Conservation Standards for Residential Central Air Conditioners and Heat Pumps; Direct final rule. Retrieved October 6, 2020, from EERE-2014-BT-STD-0048-0102 website: https://www.regulations.gov/document?D=EERE-2014-BT-STD-0048-0102.

ERTC (2014). About Ejector Refrigeration Technologies. Odessa State Academy of Refrigeration, Ejector Refrigeration Technology Center, Ukraine. website: http://www.ertc.od.ua/en/about_ert_en.html

Jiang, H., Aute, V., Radermacher, R. (2006). CoilDesigner: A General-purpose Simulation and Design Tool for Air-to-refrigerant Heat Exchangers, *International Journal of Refrigeration*, 29, 601-610.

Klein, S.A. (2020). EES – Engineering Equation Solver, Version 10.833, F-Chart Software, website: http://fchart.com.

Kornhauser, A. A. (1990). The Use of an Ejector as a Refrigerant Expander. *Proceedings of the 1990 USNCR/IIR-Purdue Refrigeration Conference*, 10–19. West Lafayette, IN.

Lawrence, N., & Elbel, S. (2013). Theoretical and practical comparison of two-phase ejector refrigeration cycles including First and Second Law analysis. *International Journal of Refrigeration*, *36*(4), 1220–1232.

Lee, W. H., Kim, Y. J., Kim, M. S., & Cho, K. S. (2000). Experimental Study on the Performance of Dual- Evaporator Refrigeration System with an Ejector. *International Refrigeration and Air Conditioning Conference.*, (503), 8.

Ling, J., Hwang,Y., & Radermacher, R. (2010). Theoretical study on separate sensible and latent cooling air-conditioning system, *International Journal of Refrigeration*, Volume 33, Issue 3, 510–520.

Tomasek, M.-L., & Radermacher, R. (1995). Analysis of a domestic refrigerator cycle with an ejector. *ASHRAE Transactions*, *101*, 1431–1438.

Wang, X., Yu, J., Zhou, M., & Lv, X. (2014). Comparative studies of ejector-expansion vapor compression refrigeration cycles for applications in domestic refrigerator-freezers. *Energy*, *70* (June 2014), 635–642.

Winkler, J., Aute, V., Radermacher, R. (2008). Comprehensive Investigation of Numerical Methods in Simulating a Steady-state Vapor Compression System, *International Journal of Refrigeration*, 31, 930-942.

ACKNOWLEDGEMENT

This material is based upon work supported by the U.S. Department of Energy, Office of Science, Building Technologies Office (BTO), FY 2019 EERE Small Business Innovation Research (SBIR), under Award Number DE-FOA-0001941.